International Journal of Thermophysics, Vol. 25, No. 3, May 2004 (© 2004)

Surface Tension Measurements on Industrial Alloys by the Drop-Weight Method

B. Vinet,[1, 2] J.-P. Garandet,[1] B. Marie,[1] L. Domergue,[1] and B. Drevet[1]

Received September 18, 2003

The drop-weight method has been successfully applied to a representative set of industrial alloys (W–Re_{26}, Mo–Re_{50}, Pt–Rh_{10}, Pt–Rh_{30}, Ti–Al_6–V_4, AISI 316 L stainless steel, INCONEL 182 and 600 alloys), with the result that very reproducible surface tension measurements ($\Delta\sigma/\sigma < 0.5\%$) have been established for these materials at the liquidus temperature. This work supports the idea that the simplicity of the drop-weight method should attract much more attention for production control or to provide reference values at the liquidus temperature, although it cannot be used for temperature coefficient measurements of the surface tension.

KEY WORDS: AISI 316 L stainless steel; drop-weight method; Inconel alloys; Mo_{50}–Re_{50} alloy; Pt–Rh alloys; surface tension; Ti_{90}–Al_6–V_4 alloy; W_{74}–Re_{26} alloy.

1. INTRODUCTION

The liquid–vapor surface energy, σ_{LV}, which pertains to the interface between the liquid (L) and its own vapor (V), is a property of interest from both theoretical and technological points of view. This property can be correlated with the atomic number in the case of pure elements, and consequently with numerous other thermophysical properties, as recently discussed for the solid–liquid interface energy [1]. The liquid–vapor surface energy, simply called the surface tension σ, plays a central importance in wetting phenomena and has to be considered for modelling or controlling material processing by liquid routes [2]. Among the several

[1] Commissariat à l'Énergie Atomique, Département des Technologies pour les Énergies Nouvelles, 17 rue des Martyrs, 38054 Grenoble Cedex 09, France.
[2] To whom correspondence should be addressed. E-mail: vinet@chartreuse.cea.fr

0195-928X/04/0500-0869/0

techniques developed for determining the surface tension of liquid metals, the sessile drop and maximum bubble pressure methods have been frequently applied as they allow the measurement of the temperature coefficient $d\sigma/dT$ (or σ') [3]. Introduced around 1980, the oscillating drop method offers the possibility to realize measurements on both the stable and metastable liquid states using containerless processing by electromagnetic [4], electrostatic [5], or aerodynamic [6] levitation techniques. Under microgravity conditions, the drop is spherical and simple formulas can be used to derive the surface tension from the oscillation spectrum [7].

Not suitable for determining temperature coefficients, at least when applied to droplets formed at the extremity of a pendant wire, the drop-weight method has been restricted in practice to reactive and high-melting point pure metals, as the conventional techniques were inapplicable. In a previous work, we have reported accurate surface tension data at the melting temperature (or σ^{m}) for pure refractory metals in the course of our drop-tube experiments [8]. Indeed, undercooling experiments realized by letting single droplets fall within the 48-m high Grenoble drop-tube required the pendant-drop configuration to prepare the studied samples. On the one hand, it is often assumed that the drop-weight method cannot be applied to alloys, as they show an interval of solidification. On the other hand, successful drop-tube experiments have been realized on many refractory alloys [9], in a context in which a perfect droplet release is prerequisite for deep liquid undercooling. In this study, we have explored the ability for the drop-weight method to deliver accurate values of the surface tension for alloys, by taking into consideration a representative set of industrial products (W–Re_{26}, Mo–Re_{50}, Pt–Rh_{10}, Pt–Rh_{30}, Ti–Al_6–V_4, AISI 316 L stainless steel, INCONEL 82 and 600 alloys).

2. EXPERIMENTAL APPROACH

The drop-weight method, initially introduced by Tate [10], has been widely applied to organic liquid droplets produced at the extremity of a capillary tube [11]. This configuration has also been used by Matuyama [12] for studying low melting point metals, but can not be considered at elevated temperatures. In the latter case, one has to form droplets by heating the lower end of a pendant rod (or wire). Consequently, this configuration is containerless but only provides data at the melting temperature T_m. The droplet detaches itself from the rod, when the surface tension can no longer balance its increasing weight. Through this method, σ^{m} measurements are based on the release conditions written as

$$\gamma = \frac{mg^0}{2\pi r^0 \alpha F}, \tag{1}$$

where m is the mass of the collected drop, g^0 is the gravitational acceleration, r^0 is the radius of the cylindrical wire at room temperature, and α is the ratio of the wire diameters between working (melting) and ambient temperature. In practice, this ratio is derived from the solid densities at the corresponding temperatures, respectively, $\rho_{\mathrm{sol}}^{\mathrm{m}}$ and ρ_{sol}^{0} (Eq. (2a)). Furthermore, F is the Harkins' empirical factor [13] which is tabulated as a function of $\delta = \alpha r^0 / V^{1/3}$ where V is the volume of the detached droplet (i.e., the ratio of the droplet mass to the liquid density ρ_{liq} at T_{m}). It was later shown that the physical origin of this factor lies within the hydrostatic pressure effect overlooked in the original work of Tate. Taking this pressure effect into account, we were able to show [14] that the discrepancy between experimental and theoretical values for F is less than 0.25% for F values around 0.8 (i.e., $2r^0$ about 1–2 mm). Since the mass is determined with great accuracy, the ultimate limit for the method is associated with the small fluctuations of the wire diameter controlled with a caliper square. This explains why this method allows high reproducibility of σ^{m} provided a well designed wire can be procured. For alloys, each density (ρ_{sol}^{0}, $\rho_{\mathrm{sol}}^{\mathrm{m}}$, and ρ_{liq}) is calculated from the values corresponding to the pure elements assuming the additivity of volumes [Eq. (2b)], where x_i is the mass percentage of element i in the alloy. The volume additivity hypothesis is a convenient simplification, but its validity may be questionable. However, it is important to note that the σ^{m} values formerly published in the literature can also be re-calculated using a new set of densities, provided a more accurate determination becomes available, if the original set is indicated as well as the droplet mass and the rod diameter.

$$\alpha = \left(\frac{\rho_{\mathrm{sol}}^{0}}{\rho_{\mathrm{sol}}^{m}}\right)^{1/3}, \tag{2a}$$

$$\rho = \frac{\sum m_i}{\sum v_i} = \frac{100}{\sum x_i / \rho_i} \tag{2b}$$

In practice, melting is realized by electron bombardment heating, as introduced by Calverley [15] (Fig. 1a). The current I ($\approx$8A) heats the cathode (Joule effect) and promotes thermo-electronic emission (Dushman–Richardson effect); melting is obtained with high efficiency when applying a negative voltage (<1.5 kV). A reduction-geared motor, giving motorized speeds ($a \approx 2\,\mathrm{mm \cdot min^{-1}}$), moves the wire downward over a maximum distance of 220 mm. When the experiment proceeds smoothly, the solid–liquid interface remains fixed with respect to the cathode. The overheating

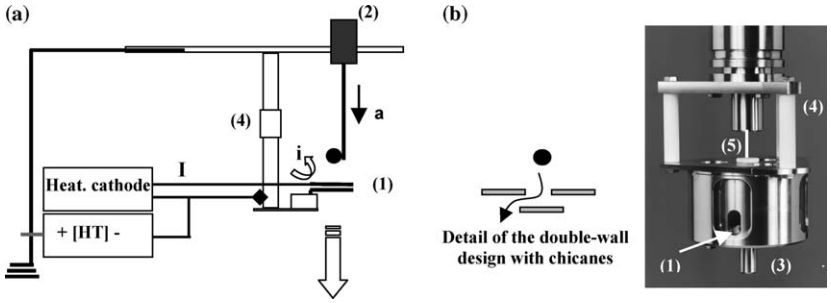

Fig. 1. (a) Schematic for electron bombardment melting and (b) picture of the melting furnace: (1) cathode, (2) reduction geared motor, (3) double-wall chamber with 100 mm diameter (see detail), (4) insulating columns, (5) calibrated guide; i is the electronic current.

δT, estimated from the existing temperature gradients within the drop, is generally very small, of the order of 20 K at most for refractory metals (see also Section 3). The elaboration, realized either under ultra-high (UHV) or secondary vacuum conditions takes place in a double-wall chamber with chicanes to facilitate an efficient evacuation of the melting zone together with protection of the facility (Fig. 1b). The wire gets into the chamber through a calibrated guide to suppress any vibration of the wire. A mass spectrometer gives partial pressures of some gases and for sintered wires, H_2 is often the primary species detected.

3. TESTS ON PURE METALS AND ADDITIONAL COMMENTS

In the case of refractory metals and alloys, σ^{m} measurements deduced from the drop-weight method have been correlated with solidification information obtained from well-characterized solidified droplets (e.g., the level of liquid undercooling prior to solidification). In lower melting-point materials, the crushed droplets are collected in a receptacle placed below the point of the release, and no control of the solidification conditions is possible. The basic studies on refractory metals and alloys were thus particularly useful to give evidence on the harmful action played by the entrapped gases in the molten volume originating from the sintered wires produced by powder metallurgy. Indeed, violent outgassing during melting causes a catastrophic spread of masses in the case of tungsten [8]. When perfect outgassing occurred, identical values ($\Delta\sigma < \pm 0.010\,\mathrm{J \cdot m^{-2}}$) were found with data obtained by authors using gas-free specimens (i.e., zone-melted rods). The materials studied in our institute include W, Re, Ta, Nb, Ir, and Zr [8] and Ti, V, and Hf [16]. As a new

example, we have measured in the course of this work the surface tension of pure platinum (Table I), before studying Pt–Rh alloys. The determined value ($1.72\,J\cdot m^{-2}$) is quite close with that proposed by Martsenyuk and Ivaschenko ($1.71\,J\cdot m^{-2}$) for zone-melted rods [17]. The agreement with the work of Martsenyuk and Ivaschenko is remarkable since the two determinations have been performed on samples having very different diameters (0.5 and 4.9 mm). Generally, the entrapped gases have a mechanical effect, leading statistically to early detachments (lower σ^m values). We observed that the higher the pumping efficiency in the melting zone, the lower the spread of masses δm (standard deviation). As a matter of fact, a comparison of experiments on ≈ 1 mm titanium wires indicates the narrower the spread of masses, the higher σ^m, namely $1.42\,J\cdot m^{-2}$ ($\delta m/m = 1.7\%$),

Table I. Summary of Surface Tension Measurements[a]

Alloys	Details and comments	ρ_{Liq}	α
W–Re_{26}	$2r^0$ = 0.99 mm, recommended value: $2.47\,J\cdot m^{-2}$ 31 elaborated droplets (see Fig. 2b) ▶ 0.6797 g	16.60	1.036
Mo–Re_{50}	$2r^0$ = 0.79 mm, 1 droplet (0.5185 g): σ^m = $2.27\,J\cdot m^{-2}$ $2r^0$ = 0.99 mm, 1 droplet (0.6378 g): $\sigma^m = 2.28\,J\cdot m^{-2}$	10.30	1.025
Pt	$2r^0 = 0.25$ mm, recommended value: $1.72\,J\cdot m^{-2}$ run 1: 3 droplets, $m* = 0.2474$ g run 2: 3 droplets, $m* = 0.2478$ g ◣ 0.2476 g	18.9	1.020
Pt–Rh_{10}	$2r^0$ = 0.50 mm, recommended value: $1.74\,J\cdot m^{-2}$ run 1: 3 droplets, $m* = 0.2507$ g run 2: 3 droplets, $m* = 0.2511$ g run 3: 3 droplets, $m* = 0.2511$ g ◣ 0.2510 g	17.7	1.019
Pt–Rh_{30}	$2r^0$ = 0.50 mm, recommended value: $1.76\,J\cdot m^{-2}$ run 1: 2 droplets, $m* = 0.2550$ g run 2: 3 droplets, $m* = 0.2552$ g ◣ 0.2551 g	15.60	1.019
$Ti_{90}Al_6V_4$	$2r^0$ = 1.47 mm, recommended value: $1.53\,J\cdot m^{-2}$ 4 droplets (0.4207, 0.4209, 0.4225, 0.4250) g ▶ 0.4223 g	4.06	1.014
AISI 316 L	$2r^0$ = 1.47 mm, recommended value: $1.77\,J\cdot m^{-2}$ 5 droplets (0.7049, 0.7057, 0.7063, 0.7063, 0.7067) g ▶ 0.7060 g	6.98	1.027
INCONEL 600	$2r^0$ = 0.95 mm, recommended value: $1.70\,J\cdot m^{-2}$ 4 droplets (0.4604, 0.4628, 0.4635, 0.4640) g ▶ 0.4627 g	6.93	1.027

Table I. (*Continued*)

Alloys	Details and comments	ρ_{Liq}	α
INCONEL 182 (high Fe)	(2909) $2r^0$ = 2.58 mm, recommended value: 1.60 J · m^{-2} 4 droplets (0.9740, 0.9745, 0.9829, 0.9840) g ▶ 0.9788 g (2910) $2r^0$ = 2.60 mm, recommended value: 1.57 J · m^{-2} 3 droplets (0.9628, 0.9636, 0.9672) g ▶ 0.9645 g (2911) $2r^0$ = 2.60 mm, recommended value: 1.60 J · m^{-2} 6 droplets (0.9784, 0.9805, 0.9828, 0.9871, 0.9913, 0.9944) g ▶ 0.9843 g	7.24	1.027
INCONEL 182 (low Fe)	(4806) $2r^0$ = 1.2 mm, recommended value: 1.33 J · m^{-2} 5 droplets (0.4324, 0.4335, 0.4339, 0.4354, 0.4454) g ▶ 0.4361 g (5566) $2r^0$ = 2.38 mm, mean value: 1.31 J · m^{-2} 7 droplets (from 0.714 to 0.767 g) ▶ 0.7348 g	7.42	1.027

[a] Liquid density in g·cm^{-3} ; for alloys, each density is calculated from the values corresponding to the pure elements assuming the additivity of volumes.

1.51 J · m^{-2} ($\delta m/m = 0.7\%$), and 1.52 J · m^{-2} ($\delta m/m = 0.3\%$, our work [17]). The entrapped gases have also an additional effect on the droplet temperature. Indeed, for a steady applied power, the interruption of the droplet feeding process causes no detectable upward movement of the molten volume, in agreement with the idea of a small overheating δT (see Section 5). Nonetheless, peaks of the electronic current may translate into a temporary increase of δT, as the entrapped gases cause a thermal resistance (Fig. 2a). When the bubble bursts, the droplet suddenly goes up to accommodate its own excess of δT. Through this effect, the true critical mass can be exceeded (σ^m overestimation).

Due to an ever possible effect of active surface impurities, the higher experimental values are often preferred in this field on the argument that they shall be closer to the true value for totally pure metals. However, this may not always be the case, as emphasized by a critical approach of Allen's work on refractory metals [18]. Allen proposed, e.g., for Re a σ^m value of 2.75 J · m^{-2} instead of 2.52 J · m^{-2} from our measurements. In fact, Allen's data are a mixture of measurements realized by both drop-weight and pendant-drop methods. In the latter method, σ^m is deduced from pictures of the pendant profiles; the overall accuracy is thus lower

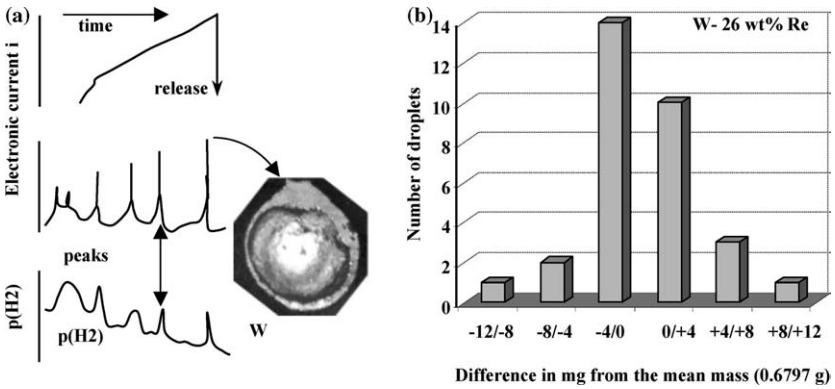

Fig. 2. (a) Characteristic behaviors displayed by the electronic current i during elaboration: (top) electronic current increases progressively till droplet releases; (below) formation of bubbles within the pendant volume (picture) leads to a succession of peaks well connected with jumps of the partial hydrogen pressure $p(H_2)$; (b) Spread of the mass per boxes of 4 mg for 31 elaborated W–Re_{26} droplets exhibiting the same undercooling ($\approx$ 650 K).

compared to the case where only a mass has to be measured. Besides, a possible source of systematic error is that the entrapped gasses may affect the shape of the pendant profile. Moreover, an accurate knowledge of the liquid density is needed. Another weakness is that Allen's data for the drop-weight method are deduced from an extrapolation procedure at zero rod diameters, which has no physical basis. To sum things up, if the effect of active surface impurities remains a key reason for low σ^{m} values, one has probably to consider that overestimations of the surface tension may also arise from both experimental procedure and material behavior.

The OFHC copper experiments performed in our institute suggest further comments, as this metal has been also studied by the oscillating drop method in two steps. The first measurements performed with this method [19] were extremely interesting, as leading to the highest σ^{m} value ever reported on pure copper ($1.39\,\mathrm{J}\cdot m^{-2}$). Excellent agreement with the drop-weight determination ($1.30\,\mathrm{J}\cdot m^{-2}$, our measurements) were found with the oscillating drop method after applying the required Cummings–Blackburn relation for correcting the effect of magnetic force exerted by the electromagnetic coil [20]. Although measurements reported by electrostatic levitation on refractory metals are higher compared to our measurements (+2% for Ti to +5% for Nb [5]), the value recently obtained on pure Rh by Paradis et al. [21] is in excellent agreement with that proposed by Eremenko and Naidich [22] using the drop-weight method

($1.94\,\mathrm{J}\cdot m^{-2}$; this value is considered to analyze the results obtained on Pt–Rh alloys).

4. SURFACE TENSION MEASUREMENTS ON INDUSTRIAL ALLOYS

As a preliminary remark, reported surface tension measurements by the drop-weight method are often based on a very limited number of droplets, four being the maximum in Allen's work on transition metals [18]. In the case of the W—26 wt% Re alloy delivered by Cime-Bocuze, an exceptional set of 31 weighed droplets has been elaborated leading to a spread in mass with a standard deviation of $\pm 0.4\%$ with respect to the mean (Table I and Fig. 2b). In practice, and as stated above, a limited number of droplets is acceptable if characterized by a high reproducibility of the mass. Our reference is a standard deviation $\delta m/m \leqslant 0.5\%$, and in that case, Table I gives a "recommended value" at the liquidus temperature.

Refractory alloy associating noble metals (Pt, Ir, and Rh) are available in the form of wires at different compositions since they are used as thermocouples. Measurements have been successfully performed on Pt–10 wt% Rh and Pt–30 wt% Rh alloys delivered by Engelhard–Clal (Table I). As for pure Pt, a number n of droplets were produced from the same wire (run) and collected together within the receptacle. Consequently, what is measured is the sum of the masses of the released drops, from which a mean mass m^* can be determined. This approach needs several runs to appreciate the reproducibility of the measurements. Measurements have also been realized on a Ti–6 wt% Al–4 wt% V alloy delivered by Good fellow (Table I). The four elaborated droplets lead to a surface tension of $1.53\,\mathrm{J}\cdot\mathrm{m}^{-2}$ ($\delta m/m = \pm 0.5\%$), which is exactly the same we have found for pure titanium [17]. The AISI 316 L stainless steel (T_m: 1380–1400°C) delivered by Goodfellow corresponds to a nominal composition of 68 wt% Fe, 18 wt% Cr, 10 wt% Ni, and 3 wt% Mo (balance 1%). On a total set of five elaborated droplets, the spread of masses is only 0.1% (Table I).

The study of Inconel alloys may be considered as a new challenge for the evaluation of the drop-weight method for studying industrial products as these alloys are characterized by a significant amount of impurities (balance). The spread of masses is only 0.4% for the heat-and corrosion-resistant Inconel 600 alloy. The five Inconel 182 alloys considered in the present work are used for TIG welding of Inconel 600, and a recommended value is given for all of them, except for the (5566) alloy (Table I). In fact, the large spread of masses obtained for the (5566) alloy is well connected with the difficulty to stabilize the droplets because of

the entrapped gases. Fortunately, the quite homologous (4806) rod, albeit with a smaller diameter (1.2 mm instead of 2.38 mm), leads to less scattered droplet masses (a "recommended" value is given at a similar composition). Let us recall that there should not be any effect of the rod size on the surface tension value deduced from drop-weight measurement, but that this result can only be obtained on gas-free specimens (see again the case of Pt in Section 3). In fact, the thinner the wire, the more efficient is the rod outgassing for a given pumping flow, as established from drop-tube experiments [23].

5. DISCUSSION ON SURFACE TENSION MEASUREMENTS

5.1. Physical Consistency of Surface Tension Measurements

The purpose of this paragraph is not to develop a fully satisfactory modelling of the surface tension, but only to evaluate if these well reproducible measurements are sufficiently realistic. In order to appreciate the physical consistency of the drop-weight measurements, we have estimated surface tension values derived from a proportional arithmetic addition of the pure substances' σ^{m} values. Since several alloy elements display very different atomic masses, care has been taken to consider nominal atomic percentages ($\sigma^{m}_{(nomin)}$). However, as exemplified in the case of the complete Ag–Au solid solution [24], the ideal solution model usually leads to a negative deviation from this mathematical addition rule. This is due to an enrichment of the liquid surface with the lower liquid–vapor surface energy constituents. Considering several examples given in Ref. 2, this tendency is also expected for more complex systems. Surprisingly enough, predictions made in the frame of the regular solution models, i.e., taking into account interactions between the alloy constituents, appear to be often quite close to the estimations from our simple additivity rule (e.g., small ranges of the positive and negative departures in the case of Fe–Si or Cu–Al, for instance). In other words, we are mainly led to expect that σ^{m}(exp) should be close, even though somewhat smaller, to $\sigma^{m}_{(nomin)}$, at least, if local thermodynamic equilibrium conditions are achieved.

Such a kind of trend is well established for the Pt–Rh system, which is homologous to Ag–Au. Indeed, the calculated $\sigma^{m}_{(nomin)}$ values are $1.76\,J \cdot m^{-2}$ for 10 wt% Rh (17.4 wt%) and $1.82\,J \cdot m^{-2}$ for 30 wt% Rh (44.8 wt%) as compared to experimental values of, respectively, 1.74 and $1.76\,J \cdot m^{-2}$. On the one hand the expected enrichment effect is identified by the drop-weight measurement. On the other hand, the differences in $\sigma^{m}_{(nomin)} - \sigma^{m}$ (exp) remain relatively small. In the same way, the calculated and measured surface tension values for the Ti–Al_6–V_4 alloy

are sufficiently close, respectively, 1.49 and 1.53 $J \cdot m^{-2}$ (we have considered the value of 1.05 $J \cdot m^{-2}$ recently reported by Sarou-Kanian et al. [25] for oxygen-free liquid aluminum). Our measurement is 10% higher than that obtained from the application of the oscillating drop technique, i.e., 1.39 $J \cdot m^{-2}$ [26].

Strong problems have been encountered to elaborate Mo droplets, and we have not been able to measure the surface tension under UHV conditions even on very thin sintered wires (0.3 mm). In this context, it is not surprising that significant disparities are observed between the σ^m values reported by the drop-weight technique: 1.95 $J \cdot m^{-2}$ [27], 2.08 $J \cdot m^{-2}$ [28], 2.12 $J \cdot m^{-2}$ [29], and 2.25 $J \cdot m^{-2}$ [19]. Nonetheless, well-released droplets can be obtained on Mo–Re alloys. Only two droplets have been elaborated in the course of our drop-tube experiments on the Mo–Re_{50} alloy (33.4 wt% Re), but from wires of different diameters. The surface tension measurement (2.27 $J \cdot m^{-2}$) agrees well with the calculated value (2.26 $J \cdot m^{-2}$), assuming the data obtained on zone-melted Mo rods (i.e., 2.12 $J \cdot m^{-2}$ [29]). In contrast, significant disagreement is obtained for the W—26 wt% Re alloy, as the calculated value is lower than the measured one (2.36 $J \cdot m^{-2}$ instead of 2.47 $J \cdot m^{-2}$). This difference may be because tungsten has a higher melting temperature than rhenium, but a lower surface tension (2.31 $J \cdot m^{-2}$ instead of 2.52 $J \cdot m^{-2}$).

In the case of the AISI 316 L and Inconel alloys, the σ^m estimations have been based on nominal weight percentages since (i) the atomic mass and the surface tension of the main elements are similar enough and (ii) the amount of refractory metals remains negligible. In this context, the surface tension measurement for AISI 316 L (1.77 $J \cdot m^{-2}$) is consistent with this straightforward calculation (1.81 $J \cdot m^{-2}$). Compared to the Inconel 600 alloy, the AISI 316 L stainless steel has a slightly higher surface tension (+0.07 $J \cdot m^{-2}$) due to its Mo amount as well as less possible tensio-active constituents within the unspecified 1% balance. The surface tension is typically 1.59 $J \cdot m^{-2}$ for the (2909), (2910), and (2911) Inconel 182 alloys, while it is only 1.32 $J \cdot m^{-2}$ for the (4806) and (5566) alloys. Nonetheless, chemical analysis of each ingot (Table II) leads us to observe that the (4806) and (5566) alloys are characterized by a higher content of Ni to the detriment of Fe ($\approx$ 2.5 wt% instead of $\approx$ 22 wt%) with a significant addition of Nb. For further analysis, we have estimated an ingot reference value σ^0, based on the mass percentages of the basic elements (Ni, Cr, and Fe) and of those identified with high-temperature metals (Nb, Mo, Ti, Co). This contribution appears to be quite consistent for all the studied alloys (1.71–1.77 $J \cdot m^{-2}$), especially in comparison to the range of the surface tension measurements.

Table II. Chemical Analyses (in wt%) of Inconel Alloys [28]

Alloy	Ni	Cr	Fe	$T1^a$	Nb	Mo	Ti	Co	$T2$	Others
INCO 600	64.29	15.43	19.18	98.90	0.00	0.00	0.00	0.04	0.04	1.06
INCO 182 (2909)	47.96	21.16	26.90	96.02	0.80	0.05	0.29	0.10	1.24	2.74
INCO 182 (2910)	48.14	20.80	26.83	95.77	0.89	0.05	0.54	0.10	1.59	2.64
INCO 182 (2911)	53.68	20.93	20.83	95.44	1.24	0.03	0.55	0.10	1.92	2.64
INCO 182 (4806)	72.54	19.78	2.40	94.72	1.70	0.00	0.26	0.00	1.96	3.32
INCO 182 (5566)	71.22	20.72	2.62	94.56	2.29	0.00	0.00	0.00	2.29	3.15

[a] $T1 = (\text{Ni, Cr, Fe})$, $T2 = (\text{Nb, Mo, Ti, Co})$.

Consequently, what is plotted (Fig. 3) is the difference between the measured σ^{m} value and σ^0 (ingot), used as a reference, Vs. the balance, i.e., the amount of other elements Mn, S, P, C, Si, Al, etc. We have also taken into account a typical chemical analysis for Inconel 600 [30]. The lower surface tension determined for the (4806) and (5566) alloys could be understood from a higher amount of impurities. Detail of the chemical analysis indicates that the main differences between (2909-2910-2911) and (4806) alloys involve the respective amounts of Mn (from 2.2 to 3 wt%) and of Al (from 0.03 to 0.18 wt%). Finally, the surface tension measurements do allow identification of two kinds of Inconel 182 alloys, well distinguished in terms of material behavior, recommended value, and effect of impurities.

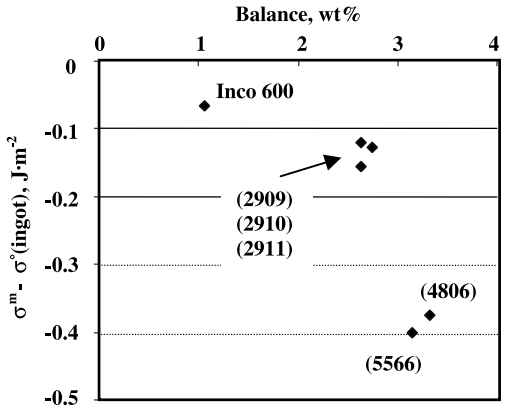

Fig. 3. Analysis of the surface tension measurements for Inconel alloys.

5.2. Temperature and Composition of Pendant Alloy Droplets

To discuss the question on the temperature of pendant alloy droplets, nucleation studies are of key importance as the presence of solid particles or surface oxides usually preclude any undercooling. In brief, successful drop-tube experiments would be hardly understood if based on undefined initial conditions pertaining to releases taking place anywhere within the interval of solidification. More precisely, experience has given great confidence with the fact that the initial temperature identifies with the liquidus temperature with an overheating δT at the most of the order of 20 K in refractory materials. This confidence comes from three main results [9]: (i) the remarkable continuity of the nucleation curve Vs. composition, (ii) the realization of statistical analyses on nucleation events, and (iii) the interpretation of the numerous phase selection phenomena occurring in these refractory systems.

For a set of 31 weighted W—26 wt% Re droplets, the time to undercool this alloy by 650 K is 1.076 s with a spread of ± 0.009 s (the interval of solidification is 200 K). Derived from the cooling rate, this spread in time corresponds to a spread in temperature of ± 5 K, which has to be "shared" between nucleation T_n and pendant drop T_i (initial) temperatures. Due to the statistical nature of nucleation [2], this spread in temperature is characteristic of the narrow one expected for homogeneous nucleation, i.e., on T_n only. We are consequently led to conclude to a high reproducibility of initial temperature T_i close to a temperature of thermodynamic significance, i.e., the liquidus temperature, keeping in mind that the presence of solid particles within the bulk is excluded through nucleation studies.

Finally, it must be pointed out that standard thermodynamic and transport considerations show that the melting front temperature is locked at the liquidus of the alloy [31–33] (noticing that the velocity of the wire is of the order of a melting/solidification rate used during directional Bridgman solidification). Moreover, an analysis of the diffusive heat transfer problem [23, 34] shows that the temperature gradients developed within the drop are very small, say of the order of 20 K at the most (refractory metal or alloy). This is further supported by the fact that convective motion, expected to be quite intense, also leads to making the drop temperature uniform. Consequently, the temperature of the pendant drop remains very close to the liquidus of the alloy, with no perturbing effect at the solid–liquid interface correlated to a chemical undercooling or overheating.

Similarly, regarding the composition field in alloy systems, it should be noted that the great originality of the pendant drop configuration is to

be based on the constant renewal of the liquid–vapor surface due to a significant evaporation rate. For instance, we are confident that environmental pollution can be safely avoided. To do so, we relied upon the approach of Camel et al. [35] in the course of a study of Marangoni flows in molten and solidifying Sn–Bi layers performed at 10^{-5} Pa. Starting from the kinetic theory of gases, it can be shown that 2 h are necessary to form an oxide monolayer for a partial pressure of oxygen of 10^{-8} Pa. In our UHV conditions, the total pressure is 10^{-7} Pa within the facility (mainly identified with the partial pressure of hydrogen) and oxygen is not detected by the mass spectrometer ($<10^{-9}$ Pa). On the one hand, the evaporation flow can be experimentally estimated by selecting a wire advancing rate low enough for the drop to stabilize. Taking into account the wire and drop diameters, we were able to show that the evaporation rate is orders of magnitudes higher than the pollution rate. As the oxide layer growth velocity is directly proportional to the ambient pressure, secondary vacuum conditions are enough to guarantee the absence of pollution from the environment.

We have to keep in mind that outgassing (case of sintered wires) is preferentially obtained for a high level of pumping flow in the melting zone that can be also optimized through the design of the heating furnace. A potential problem is that it could be argued that the evaporation rate may perturb local thermodynamic equilibrium conditions at the liquid–vapor interface. Fortunately, the kinetics of segregation of lower surface tension constituents at the interface are very fast. Indeed, the relevant transport mechanism is diffusion from an enriched zone located below the interface. As the typical transport velocity scales with the ratio of the species diffusion coefficient to the width of this enrichment zone (typically a few atomic distances), the kinetics of the mass transport phenomena are very fast (again many orders of magnitude higher than the evaporation rate), meaning that local equilibrium conditions can be considered established at all times at the liquid–vapor interface. Our conclusion is that the pendant-drop configuration is characterized by a high reproducibility in both the temperature and the composition of the material at the moment of release.

6. CONCLUSION

The pendant drop design leads to a high reproducibility of the droplet mass, with a standard deviation smaller than 0.5% often being achieved, which is a necessary condition to guarantee the validity of the surface tension measurement. The spread in masses is mainly related to the action of entrapped gases, but that can be monitored through the evolution of

the electronic current. The constant renewal of material, due to a substantial evaporation rate in clean vacuum conditions, as well as the possibility to efficiently establish local thermodynamic equilibrium conditions in the neighborhood of the detachment area through fast solute transport mechanisms in alloys, are basically the reasons for reproducibility of the liquid initial conditions expressed in terms of temperature and chemical composition (melting). From this point of view, the simplicity of the drop-weight method should attract much more attention for production control and, maybe, provide reference values at the liquidus temperature.

ACKNOWLEDGMENTS

The drop-tube experiments have been performed within the now defunct GRAMME agreement between CEA and CNES. This contribution is also part of the ESA-Thermolab project "High-Precision Thermophysical Property Data of Liquid Metals for Modelling of Industrial Solidification Processes," coordinated by H. J. Fecht (University of Ulm). The Inconel 182 alloys have been delivered by courtesy of Soudometal in the course of the PhD Thesis of L. Domergue devoted to the welding process.

REFERENCES

1. B. Vinet, L. Magnusson, H. Fredriksson, and P. J. Desré, *J. Colloid Interface Sci.* **255**:363 (2002).
2. N. Eustathopoulos, M. G. Nicholas, and B. Drevet, *Wettability at High Temperature* (Pergamon, Amsterdam, 1999).
3. B. J. Keene. *Int. Mat. Rev.* **38**:157 (1993).
4. I. Egry, S. Sauerland, and G. Jacobs. *High Temp.-High Press.* **26**:217 (1994).
5. P. F. Paradis, T. Ishikawa, and S. Yoda. *Int. J. Thermophys.* **23**:825 (2002).
6. G. Wille, F. Millot, and J. C. Rifflet. *Int. J. Thermophys.* **23**:1197 (2002).
7. I. Egry, G. Lohöfer, I. Seyhan, S. Schneider, and B. Feuerbacher, *Int. J. Thermophys.* **20**:1005 (1999).
8. B. Vinet, J. P. Garandet, and L. Cortella. *J. Appl. Phys.* **73**:3830 (1993).
9. See, for a review, B. Vinet, *Int. J. Mater. Product Technol.*, in press.
10. T. Tate, *Philos. Mag.* **21**:176 (1864).
11. See, e.g., N. Tsapis, R. Ober, A. Chaffotte, D. E. Warschawski, J. Everett, J. Kauffman, P. Kahn, M. Waks, and W. Urbach, *Langmuir* **18**:4384 (2002).
12. Y. Matuyama, *Sci. Rep. Tôhoku Imp. Univ*. **16**:555 (1923).
13. W. Harkins and F. E. Brown, *J. Am. Chem. Soc.* **41**:499 (1919).
14. J. P. Garandet, B. Vinet, and P. Gros, *J. Colloid Interface Sci.* **165**:351 (1994).
15. A. Calverley, *Proc. Phys. Soc.* **70**:1040 (1956).
16. P. S. Martensyuk and Yu. N. Ivaschenko, *Ukr. Khim. J.* **4**:431 (1973).
17. B. Vinet and J. P. Garandet, *Proc. 2nd Int. Conf. High Temperature Capillarity*, N. Eustathopoulos, ed. (Reproprint, Bratislava, 1995), pp. 223–227.

18. B. C. Allen, *Trans. Metall. Soc. AIME* **227**:1175 (1963).
19. B. J. Keene, *The Use of a Fourier Analyser for Determination of the Surface Tension of Liquid Metals by the Levitating-Drop Technique,* Report DMA (A) 56 (National Physical Laboratory, Teddington, Middlesex, United Kingdom, 1982).
20. I. Egry, S. Sauerland, and G. Jacobs, *High-Temp.–High Press*. **26**:217 (1994).
21. P. F. Paradis, T. Ishikawa, and S. Yoda, *Int. J. Thermophys*. **24**:1121 (2003).
22. V. N. Eremenko and Yu. Naidich, *Izv. Akad. Nauk. SSR OTN Met. Topliva* **6**:100 (1966).
23. B. Vinet, L. Cortella, and A. Bloch, *Trans. Mat. Res. Soc. Jpn.* **16A**:593 (1994).
24. G. Bernard and C. H. P. Lupis, *Met. Trans.* **2**:555 (1971).
25. V. Sarou-Kanian, F. Millot, and J. C. Rifflet, *Int. J. Thermophys*. **24**:277 (2003).
26. S. Schneider, I. Egry, and I. Seyhan, *Int. J. Thermophys*. **23**:1241 (2002).
27. A. I. Pekarev, *Izv. Vuz Tsvetn. Metall.* **6**:11 (1963).
28. S. Namba and T. Isobe, in *Proc. 4th Symp. Electron Beam Technology*, R. Bakish, ed. (1962), pp. 96–99.
29. V. N. Eremenko, Y. U. N. Ivashchenko, and P. S. Martsenyuk, *Teplofiz. Vys. Temp.* **18**:1326 (1980).
30. L. Domergue, Ph.D. thesis, École Centrale de Nantes, France (1997).
31. J. D. Verhoeven and K. A. Heimes, *J. Cryst. Growth* **10**:179 (1971).
32. J. D. Verhoeven and E. D. Gibson, *J. Cryst. Growth* **11**:39 (1971).
33. H. Nguyen Thi, B. Drevet, J. M. Debierre, D. Camel, Y. Dabo, and B. Billia, *J. Cryst. Growth* **253**:539 (2003).
34. B. Vinet, L. Cortella, and J. Comera, *Ann. Chim. Fr*. **15**:443 (1990).
35. D. Camel, P. Tison, and J.P. Garandet, *Eur. Phys. J. Appl. Phys*. **18**:201 (2002).